Effects of Peripapillary Scleral Stiffening on the Deformation of the Lamina Cribrosa

Baptiste Coudrillier,[1] Ian C. Campbell,[1,2] A. Thomas Read,[1] Diogo M. Geraldes,[3] Nghia T. Vo,[4] Andrew Feola,[1] John Mulvihill,[1] Julie Albon,[5,6] Richard L. Abel,[7] and C. Ross Ethier[1,2]

[1]Wallace H. Coulter Department of Biomedical Engineering, Georgia Institute of Technology and Emory University, Atlanta, Georgia, United States
[2]Atlanta VA Medical Center, Decatur, Georgia, United States
[3]Biomechanics Group, Department of Mechanical Engineering, Imperial College London, London, United Kingdom
[4]Diamond Light Source, Didcot, United Kingdom
[5]Optic Nerve Group, School of Optometry and Vision Sciences, Cardiff University, Cardiff, Wales, United Kingdom
[6]Cardiff Institute of Tissue Engineering and Repair, Cardiff University, Cardiff, Wales, United Kingdom
[7]Department of Surgery and Cancer, Imperial College, London, United Kingdom

Correspondence: C. Ross Ethier, 315 Ferst Drive NW, Atlanta, GA 30332, USA;
ross.ethier@bme.gatech.edu.

PURPOSE. Scleral stiffening has been proposed as a treatment for glaucoma to protect the lamina cribrosa (LC) from excessive intraocular pressure–induced deformation. Here we experimentally evaluated the effects of moderate stiffening of the peripapillary sclera on the deformation of the LC.

METHODS. An annular sponge, saturated with 1.25% glutaraldehyde, was applied to the external surface of the peripapillary sclera for 5 minutes to stiffen the sclera. Tissue deformation was quantified in two groups of porcine eyes, using digital image correlation (DIC) or computed tomography imaging and digital volume correlation (DVC). In group A ($n = 14$), eyes were subjected to inflation testing before and after scleral stiffening. Digital image correlation was used to measure scleral deformation and quantify the magnitude of scleral stiffening. In group B ($n = 5$), the optic nerve head region was imaged using synchrotron radiation phase-contrast microcomputed tomography (PC µCT) at an isotropic spatial resolution of 3.2 µm. Digital volume correlation was used to compute the full-field three-dimensional deformation within the LC and evaluate the effects of peripapillary scleral cross-linking on LC biomechanics.

RESULTS. On average, scleral treatment with glutaraldehyde caused a $34 \pm 14\%$ stiffening of the peripapillary sclera measured at 17 mm Hg and a $47 \pm 12\%$ decrease in the maximum tensile strain in the LC measured at 15 mm Hg. The reduction in LC strains was not due to cross-linking of the LC.

CONCLUSIONS. Peripapillary scleral stiffening is effective at reducing the magnitude of biomechanical strains within the LC. Its potential and future utilization in glaucoma axonal neuroprotection requires further investigation.

Keywords: biomechanics, phase contrast microcomputed tomography, digital image correlation, digital volume correlation

Glaucoma, the second leading cause of irreversible blindness, affects over 60 million people worldwide.[1] Intraocular pressure (IOP) plays an important role in the pathophysiology of glaucoma: Elevated IOP is a risk factor for the disease, and significant, sustained IOP reduction benefits most patients.[2,3] All treatments for glaucoma in present clinical use attempt to modulate aqueous humor fluid dynamics to reduce IOP. Unfortunately, loss of vision progresses in 25% to 45% of patients[2,4] despite reduction of IOP. Therefore, there is a critical need to develop new treatments for glaucoma not based upon the paradigm of lowering IOP.

Vision loss in glaucoma is caused by the slow and irreversible loss of retinal ganglion cell axons. Evidence suggests that biomechanical factors acting on the axons, cells, and extracellular matrix of the optic nerve head (ONH) contribute to this process.[5,6] Damage to the axons first occurs in the lamina cribrosa (LC),[7] which undergoes substantial deformation,[8] and ONH astrocytes are known to alter their phenotypic expression when subjected to mechanical insults.[9,10] These data suggest that reducing the deformation experienced by ONH tissues may be beneficial for glaucoma patients.[11-13]

Computer modeling work has shown that a major factor controlling the deformation of the LC is the stiffness of the sclera,[14,15] especially the stiffness of the peripapillary sclera.[16] These studies predicted that the LCs of eyes with stiffer scleras would deform less. Accordingly, altering the biomechanical properties of the sclera has been suggested as a potential approach to protect individuals with elevated IOP or with comparatively less stiff scleras from glaucomatous injury.[6,11-13] However, it is unclear as to whether a stiffer sclera is in fact neuroprotective. On one hand, eyes from mice with
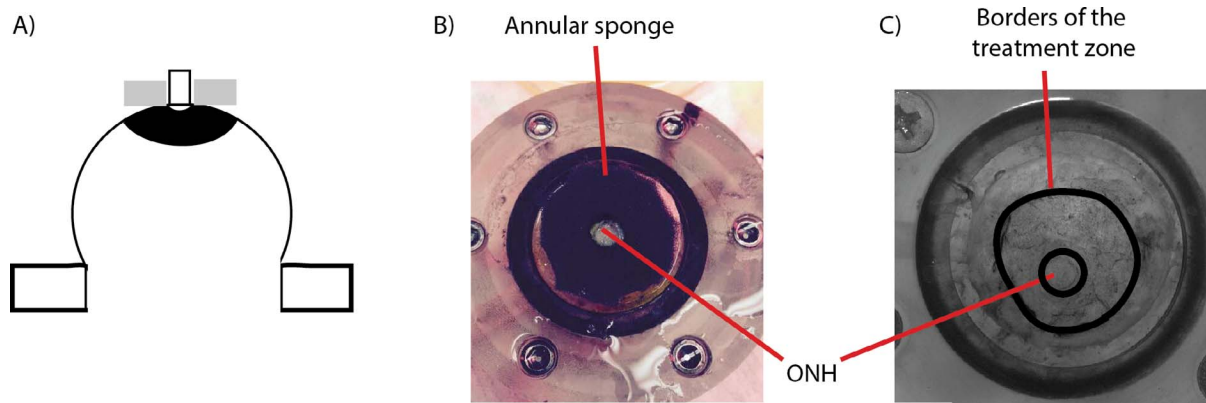
Figure 1. Scleral stiffening procedure. (A) Schematic representation of the treatment region in the peripapillary sclera. This is a side view of the specimen, glued on the holder at the limbus, with the optic nerve facing up. Note that the length of the optic nerve is exaggerated in this schematic. Only 1 mm of optic nerve was left in the experiments. The approximate treatment zone is shaded in *black* and the sponge is represented in *gray*. The sponge was not pressed onto the scleral surface. (B) Top view of the specimen during treatment, with the annular sponge placed on the peripapillary sclera around the ONH, which is visible in the center. Scleral stiffening was performed when the specimen was mounted on the pressure chamber. The annular sponge was immersed in the 1.25% (vol/vol) glutaraldehyde solution and placed around the optic nerve for 5 minutes. (C) Delineation of the treatment region after treatment, as viewed by a camera looking down on the specimen. The cross-linking solution was yellow (not visible in this black and white picture), which allowed us to trace the contours of the treatment zone.

experimental glaucoma that experienced greater scleral strains were more prone to axonal damage.[17] Further, animal studies have suggested that natural stiffening of the sclera may occur in early glaucoma as a protective response to shield the ONH from the mechanical insult caused by long-term exposure to IOP. For example, increased scleral stiffness was observed in a mouse model of experimental glaucoma using an inflation test[17] and in a monkey model of experimental glaucoma using uniaxial relaxation[18] and inflation testing.[19] A stiffer sclera has also been reported in humans with glaucoma[20,21]; however, nonlongitudinal human studies cannot determine if these patients had increased scleral stiffness prior to glaucoma or if it was a response to the disease. On the other hand, mice with experimentally induced glaucoma whose scleras were chemically stiffened exhibited more axon loss compared to experimental glaucoma mice whose scleras were left unstiffened.[22] Further research is needed to elucidate the neuroprotective effects, if any, of increased scleral stiffness in glaucoma. An essential part of this research is the quantification of how altering scleral stiffness impacts LC deformation.

Stiffening collagen-rich tissues such as the sclera or the cornea can be achieved by treatment with cross-linking agents. For instance, physical corneal collagen cross-linking via ultraviolet (UV)-activated riboflavin treatment is now commonly used to prevent the progression of keratoconus,[23] and scleral cross-linking with riboflavin is currently being tested in animal models as a treatment for myopia.[24] Treatment of the sclera with riboflavin/UV or chemical agents such as glutaraldehyde or glyceraldehyde resulted in increased scleral stiffness as measured with uniaxial tensile testing.[25] A recent study by Thornton et al.[26] showed that treatment of the peripapillary sclera with glutaraldehyde caused a 3-fold increase in scleral stiffness and a large decrease in LC tensile deformation. However, the authors used relatively low-resolution tools to measure the mechanical behavior of the sclera and the LC, and more experimental studies are needed to assess the effects of scleral stiffening on LC deformation. Here, we have quantified the effects of peripapillary scleral stiffening on the three-dimensional (3D) deformation of the LC using high-resolution imaging and deformation mapping techniques.

MATERIALS AND METHODS

Overall Approach

The overall goal of this study was to estimate the effects of glutaraldehyde-induced peripapillary scleral stiffening on the deformation, or "strain" of the LC. Although we do not propose glutaraldehyde as a viable in vivo stiffening agent due to biocompatibility limitations, it was suitable for use in this proof-of-principle study as it is known to produce significant stiffening of collagenous tissues in short time frames.[26] After verifying that glutaraldehyde delivery was localized to the sclera and did not diffuse into the LC, we quantified the relative scleral stiffening caused by a superficial application of a 1.25% glutaraldehyde solution to the peripapillary sclera. Scleral specimens were subjected to inflation testing before and after glutaraldehyde treatment, and peripapillary scleral deformation was measured with digital image correlation (DIC). We refer to this study as experiment A in the remainder of the paper. Next, we evaluated the effects of scleral stiffening on deformation within the LC. The 3D structure of the LC was imaged at increasing levels of IOP using phase-contrast microcomputed tomography (PC μCT), and IOP-induced LC strains were computed with digital volume correlation (DVC). We refer to this study as experiment B in the remainder of the paper.

Specimen Preparation

Porcine eyes, obtained from local slaughterhouses within 24 hours of death, were divided into two experimental groups. The first group, consisting of 14 eyes from animals aged 24 months (Holifield Farm, Inc., Farmington, GA, USA), was used in experiment A, conducted at Georgia Institute of Technology, Atlanta, Georgia. The second set consisted of five eyes from animals aged 5 months (Elmkirk, London, UK) and was used in experiment B, conducted at Diamond Light Source synchrotron (Didcot, UK). All eyes were stored in a moist chamber at 4°C prior to dissection, which occurred within 72 hours post mortem, within the time frame over which scleral properties are known to be preserved.[27] Both sets of eyes were prepared using the protocol described in Coudrillier et al.[28] In brief, the eyes were cleaned of extraorbital fat and muscles, hemisected, and glued with cyanoacrylate at the corneal/scleral limbus onto a resin holder (Fig. 1A). The mounted specimens were
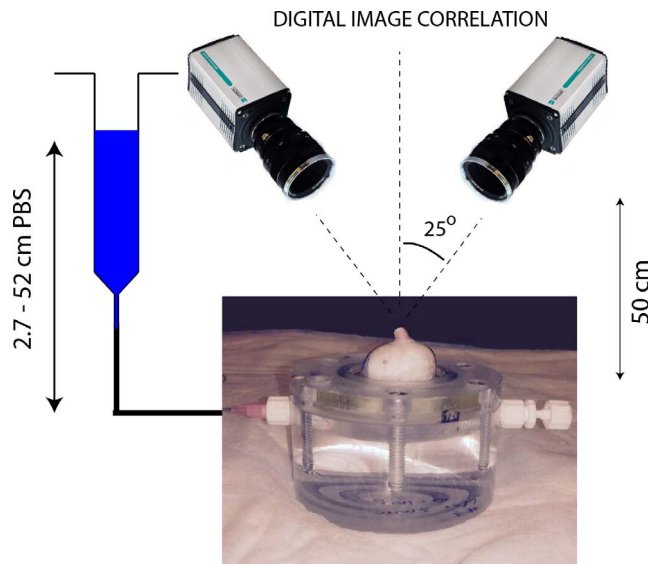
DIGITAL IMAGE CORRELATION

FIGURE 2. Schematic representation of the experimental setup used for digital image correlation. The sclera was securely attached to an inflation chamber, which was connected to a syringe filled with PBS, the height of which was manually adjusted to control pressure in the chamber. Two cameras imaged the deforming sclera during inflation at a rate of 1 Hz. The inflation chamber was immersed in a PBS bath, not shown in this figure. Note that a relatively long optic nerve was initially left on the eye for this photo. It was cut to a length of approximately 1 mm before starting the inflation test to ensure quality correlation in the DIC measurements of the peripapillary scleral deformation.[33]

then secured onto a pressure chamber (Fig. 2) filled with isotonic phosphate-buffered saline (PBS). Intraocular pressure could be hydrostatically adjusted by controlling the vertical position of a PBS-filled reservoir. The mounted eye was then immersed in a PBS bath to maintain constant hydration and environmental temperature during testing. Eyes were inflated to 15 mm Hg for 20 minutes to ensure the absence of leaks at the glued interface between the hemisected eye and the holder before starting the scleral or LC deformation measurements. No further preconditioning tests were performed on the specimens.[28,29]

Scleral Cross-Linking

Peripapillary Scleral Treatment. Scleral cross-linking was achieved by topical application of a 1.25% (vol/vol) solution of glutaraldehyde (dilution of a 25% biological-grade solution [Electron Microscopy Science, Hatfield, PA, USA] in PBS) fluorescently labeled by addition of fluorescein sodium salt (Sigma-Aldrich Corp., St. Louis, MO, USA) to reach a final concentration of 0.33 mM. The cross-linking solution had a bright yellow color, which allowed us to precisely track the region of the scleral surface treated with glutaraldehyde and ensure that no drops of fixative-containing solution ran down the scleral surface from the sponge. In more detail, an annular sponge made of synthetic foam was immersed in this glutaraldehyde solution, blotted on absorbent paper to remove excess solution that might run down the scleral surface, and placed on the external surface of the peripapillary sclera for 5 minutes, as shown in Figure 1A.[26] After treatment, the scleral surface was immersed in PBS three times to wash the excess glutaraldehyde from the surface. We did not rely on the yellow stain caused by fluorescein to measure lateral diffusion of glutaraldehyde. This was done in another experiment described below.

Validation of the Cross-Linker Application. Glutaraldehyde, which has a relatively small molecular weight (100.12 $g \cdot mol^{-1}$), is expected to diffuse through the peripapillary sclera upon application. With enough time, glutaraldehyde could diffuse into the LC. From the physics of diffusion, we expected that if glutaraldehyde reached the LC, the concentration of glutaraldehyde would be larger in the LC regions closest to the peripapillary sclera (i.e., the periphery of the LC versus the center of the LC), and the concentration of glutaraldehyde in the LC would increase with time until reaching an equilibrium value.

It was important to verify that the LC remained unstiffened after 5 minutes of scleral exposure to 1.25% glutaraldehyde, since the point of this study was to evaluate the effects of scleral stiffening alone on LC deformations. The diffusion coefficients of glutaraldehyde in the sclera and the LC are unknown, and the concentration of glutaraldehyde within the LC after treatment could not be numerically estimated. Thus, we instead used the autofluorescence of tissue fixed with glutaraldehyde as a marker to experimentally determine the maximum concentration of glutaraldehyde, if any, present in the LC. This was done in the following two steps.

Overnight Incubation of LCs in Glutaraldehyde (Step 1). In the first step, we determined a "dose–response" curve between the glutaraldehyde concentration in the LC and tissue autofluorescence. To do so, we measured the fluorescence of LCs incubated overnight in solutions with different concentrations of glutaraldehyde, with the expectation that overnight incubation would be long enough for the concentration of glutaraldehyde to have reached an equilibrium value across the LC. Eleven fresh porcine eyes were dissected to isolate the ONH region. The retina was gently excised but the choroid was left on the specimen. Each specimen was then incubated overnight in a different concentration of glutaraldehyde solution, varying from 1.25% (stock solution) to 0.01%. One control specimen was incubated in PBS. We did not use fluorescein in this experiment as fluorescein has a larger molecular mass and would diffuse more slowly within the sclera. Following incubation, all excess glutaraldehyde solution was removed by immersion in PBS for 1 hour. The specimens were then embedded in Tissue-Tek optimal cutting temperature medium (OCT; Sakura Finetek, Torrance, CA, USA) and snap frozen at −80°C. For each specimen, eighteen 20-μm-thick cryosections through the LC were cut on a CryoStar NX70 cryostat (Microm International GmbH, Dreieich, Hessen, Germany), three of which were randomly selected per eye and imaged using a ×10 objective lens on a Zeiss LSM 700-405 microscope (Jena, Thuringia, Germany) with 555-nm laser excitation. The autofluorescence of glutaraldehyde-fixed tissue is maximally excited at 540 nm, with an emission peak at 560 nm.[30] The confocal pinhole was set to 1 AU (12.3 μm), the laser power set to 2%, the digital offset to 0, and the digital gain set to 4.

We expected that the autofluorescence of the LC exposed to glutaraldehyde would depend on the concentration of glutaraldehyde in the incubation solution. As a measure of tissue autofluorescence for each concentration, we determined the maximum detector gain that would saturate a few pixels of the brightest optical section of each slice (as seen on the saturation color map, Zeiss, Zen), and plotted this gain versus glutaraldehyde concentration to obtain a suitable "gain–concentration curve."

Scleral Treatment With 1.25% Glutaraldehyde Treatment (Step 2). In the second step, we used the above-determined curve to estimate the concentration of glutaraldehyde in the LC caused by peripapillary scleral stiffening. Our specific goal was to demonstrate that no glutaraldehyde had reached the LC after

5 minutes of exposure via the sponge on the peripapillary scleral surface. The peripapillary scleral surface of seven different porcine eyes was treated with 1.25% glutaraldehyde for times varying between 5 minutes and 6 hours following the protocol shown in Figure 1. For treatment times longer than 1 hour, the annular sponge was soaked in glutaraldehyde hourly to ensure that the supply of cross-linking solution was not depleted. After treatment, the ONH region was dissected and washed for 1 hour in PBS. Transverse cryosections of the LCs were prepared and imaged following the protocol described in step 1. In this experiment, diffusion of glutaraldehyde occurs between the peripapillary sclera and the LC (initial concentration = 0%). Similarly to the procedure in step 1, we measured the maximum detector gain that saturated a few pixels of the peripheral and central LC, and used the curve generated in step 1 to estimate the evolution of the concentration of glutaraldehyde in those regions versus treatment time.

Experiment A: Measurement of the Relative Scleral Stiffening

Digital Image Correlation. Fourteen posterior porcine scleral shells were subjected to inflation testing to measure their mechanical behavior in response to elevation of pressure. The scleral shells were mounted on the inflation chamber shown in Figure 1. Surface displacement maps of the sclera were computed using DIC, a technique previously applied to measure the deformation of bovine[31] and human[32] sclera. Prior to testing, the sclera was air brushed with black Indian ink to create a contrast pattern for deformation tracking. Two cameras, located approximately 50 cm above the inflation chamber with a 25° stereo angle, acquired pictures of the deforming sclera at a rate of 1 Hz (Fig. 2). Test image pairs were analyzed with a 3D DIC software package (Istra 4D 4.4.1; Dantec Dynamics, Holtsville, NY, USA) to compute full-field displacements of the scleral surface (30.7 μm/pixel, facet size = 51 pixels, overlap = 21 pixels). The DIC software includes a compensation method to correct for optical distortions due to change in refraction indices at the surface of the PBS bath. Displacements were smoothed using cubic splines (grid reduction factor = 4) before computing the 2D surface Green-Lagrange strain tensor and principal strains with the algorithm implemented in Istra 4D. The two principal strains represent the maximum and minimum stretches of an elemental scleral surface. The uncertainty in the strain calculation was estimated by taking two sets of stereo images of the equilibrated sclera 1 second apart[31] without varying IOP and correlating the second image set with the first to compute displacements and strains. In this scenario, we expect the computed strains to be uniformly zero. The strain uncertainty was defined as the standard deviation of the computed first principal strain over the entire peripapillary sclera, defined as the region spanning a radial distance from 1.5 to 6 mm from the center of the ONH. The uncertainty was estimated to be 0.5 millistrain.

After uncertainty estimation, the specimen (not yet treated with glutaraldehyde) was allowed to equilibrate for 20 minutes at 2 mm Hg before beginning the inflation test. The pressure was increased from 2 to 38.5 mm Hg by steps of 7.3 mm Hg (i.e., 6 steps of 10 cmH$_2$O) and maintained at each pressure step for 10 seconds. The pressure was then lowered and held at the baseline pressure of 2 mm Hg. The inflation chamber and specimen were taken out of the PBS bath, and the peripapillary sclera was treated for 5 minutes with 1.25% glutaraldehyde using the protocol shown in Figure 1. After three washes of any excess glutaraldehyde with PBS, the PBS bath was filled with fresh PBS and the inflation test was repeated on the treated specimen. Note that the treatment and

the washes did not alter the speckling pattern, and that the same camera calibration and specimen orientation were used to measure the mechanical behavior of the specimen before and after treatment.

Scleral Stiffening Quantification. The relative scleral stiffening at pressure step p was calculated as:

$$S_p = 100 \times \frac{\varepsilon^p_{\text{untreated}} - \varepsilon^p_{\text{treated}}}{\varepsilon^p_{\text{untreated}}}, \qquad (1)$$

where $\varepsilon^p_{\text{untreated}}$ and $\varepsilon^p_{\text{treated}}$ are the first principal strains (i.e., maximum tensile deformation) averaged over the entire peripapillary sclera at pressure p before and after treatment, respectively. $\varepsilon^p_{\text{untreated}}$ and $\varepsilon^p_{\text{treated}}$ were computed from the strain profile obtained in the last stereo images acquired at pressure step p. The specimen had to be taken out of the PBS bath for treatment and therefore was not in the exact same orientation/location before and after treatment. To prevent error arising from registration of the specimens, we used an axisymmetric region centered on the optic nerve (ON) for strain averaging, after manual registration of the center of the ON between the treated and untreated scans. The peripapillary sclera was defined as the disc-shaped region lying between 1.5 and 6 mm from the ONH center. Material points with poor correlation values were not included in the strain average over this region; however, because we used the same speckling pattern, these regions were nearly identical for the treated and untreated specimens, so that treated/untreated comparisons were valid.

As a control experiment, we recorded two inflation tests 15 minutes apart for six specimens incubated in PBS instead of glutaraldehyde. We compared the relative stiffening to zero at each pressure using a 1-sample t-test with a Bonferroni correction (adjusted P value of 0.01).

Experiment B: IOP-Induced Strain in the LC

Phase-Contrast Microcomputed Tomography. The effects of IOP on the 3D deformation of the LC were measured with phase-contrast PC μCT on beamline I12, Joint Engineering, Environment and Processing at Diamond Light Source.[34] The experimental protocol for PC μCT was described in a previous publication[28] and is briefly summarized here. A highly coherent x-ray beam was directed toward the ONH region of a hemisected eye mounted on a turntable (Fig. 3). The phase shift caused by the interaction of the x-rays with the tissues of the ONH was transformed into intensity variations and recorded using a charge-coupled device detector with an effective voxel size of 3.2 μm placed 2 m behind the specimen. We acquired 3600 projections of the ONH region and used an exposure time of 5 ms per projection (total scan time at each pressure ~90 seconds). The reconstructed scans encompassed a 7- $\times$ 7- $\times$ 7-mm^3 region centered on the LC.[35] To reduce the file size of the image volume used for image processing, the images were down-sampled by a factor of 2 (Matlab [Mathworks, Natick, MA, USA] command imresize). The effective voxel size of the down-sampled image volume was 6.4 μm. Phase-contrast microcomputed tomography scans were recorded at three different levels of IOP: 4, 15, and 30 mm Hg. The specimens were equilibrated at each pressure for 15 minutes before starting the scan to minimize motion caused by creep, which would manifest as a smearing artifact and ruin the scan. After acquiring the scan at 30 mm Hg, the pressure was lowered and held at the baseline pressure of 4 mm Hg. The PBS bath was emptied, and the peripapillary sclera was treated with 1.25% glutaraldehyde for 5 minutes as indicated in Figure 1. The sponge was then removed; excess glutaraldehyde was washed off; the bath was refilled with fresh PBS; and three
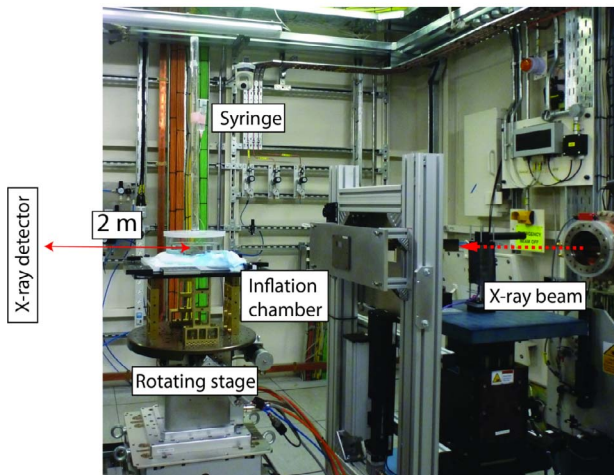
PHASE-CONTRAST MICRO-COMPUTED TOMOGRAPHY

FIGURE 3. Experimental protocol for PC μCT. The inflation chamber (shown in Fig. 2) was immersed in a PBS bath, and the entire apparatus was placed on a rotating stage. An x-ray beam, produced by synchrotron radiation, was directed toward the ONH region. The x-ray detector was placed 2 meters behind the specimen. For PC μCT, a few millimeters of optic nerve were left on the eye.

scans at 4, 15, and 30 mm Hg were acquired using the same specimen.

Digital Volume Correlation. The IOP-induced deformation of the LC was computed using DVC, which is a feature-tracking technique similar to DIC except that DVC operates on full image volumes instead of 2D images of surfaces. We recently characterized the application of this method to study deformation of the porcine LC.[28] Briefly, the image volumes acquired at 15 and 30 mm Hg were correlated with the image volume acquired at 4 mm Hg to compute the six independent components of the spatially varying Green-Lagrange strain tensor using the software DaVis 8.1.3 (LaVision, GmbG, Goettingen, Germany). The subvolume size used was 20 × 20 × 20 voxels, with a 75% overlap, which resulted in a strain accuracy of 20 microstrain.[28] DaVis computes the correlation value for each subvolume, which is a number between 0 and 1, with 1 corresponding to a perfectly correlated subvolume and 0 corresponding to a subvolume that could not be correlated. We used this value as a quality check to remove regions of the LC that were poorly correlated, defined as subvolumes with correlation value lower than 0.7.[36] The DVC displacements were imported into Matlab and smoothed using cubic splines (csaps function, smoothing parameter 0.999 for all displacement components). The Matlab gradient function was applied to compute the derivatives of the displacements for the Green-Lagrange strain formulation. The Green-Lagrange strain tensor was then diagonalized to compute its three principal strain components, as well as directions. Those are three mutually perpendicular directions of pure extension or contraction.

Effects of Scleral Stiffening on the Deformation of the LC. The effects of stiffening the peripapillary sclera on the deformation of the LC at pressure step p were evaluated using equation 1, where $\varepsilon^p_{untreated}$ and $\varepsilon^p_{treated}$ were the first principal strains averaged over the entire LC, both computed at pressure p. A voxel selection mask of the LC was manually created for each of the five specimens used in this study to eliminate the sclera, the prelaminar tissues, and postlaminar tissue from analysis. The selection mask was created based on the following criteria. The retina and the peripapillary sclera have limited natural anatomic features, which resulted in those

regions being poorly correlated with DVC. Therefore, the anterior surface of the LC and the scleral canal were easily detectable on maps of the DVC correlation value. The density of collagen was slightly lower in the pial septae than in the LC.[28] This caused a decrease in the correlation value at the border between the LC and pial septa, which we used to delineate the posterior boundary of the LC. The same mask was used for the treated and untreated specimens. This was possible because the masks were constructed following the same anatomic features observed in the treated and untreated specimens and using the value of the correlation coefficient in the LC, which depends on tissue density and μCT parameters, both unchanged by treatment. In addition, the specimen was not displaced or rotated during treatment. The glutaraldehyde was applied to the specimen while resting on the μCT stage. Therefore, the position and orientation of the LC and its mask were identical in the treated and untreated specimens at the baseline pressure. In other words, the strains were averaged over the same volume of LC tissue in the treated and untreated specimens.

RESULTS

Diffusion of Glutaraldehyde

Overnight Incubation of LCs in Glutaraldehyde (Step 1). Fluorescence due to glutaraldehyde fixation was observed much more strongly from tissue within the pores of the LC as compared to the collagenous beams (Fig. 4A), likely due to the well-known tendency of neurons to autofluoresce strongly after aldehyde fixation.[37] Since our goal was simply to determine if there was any glutaraldehyde reaching the LC, we focused only on the signal from the pores as the most sensitive measure. At 550 nm, autofluorescence of the untreated specimen was very weak (i.e., could be observed only at a very high gain of >900), and was located primarily in the collagen beams of the LC (Fig. 4B).

For each glutaraldehyde bath concentration, it was possible to determine the optimal detector gain to visualize autofluorescence from the LC (Fig. 4). For this optimal gain, only a few pixels of the image were saturated (Fig. 4A, left). For each glutaraldehyde concentration, the standard deviation of the optimal detector gain over the LC was relatively small (Fig. 5), suggesting that the glutaraldehyde reached a near-uniform spatial distribution in tissue outside the LC beams after overnight incubation. We observed three different states of fluorescence while developing the gain–concentration curve. At high concentrations of glutaraldehyde (>0.025%), autofluorescence was observed only in the pores when the gain was set to a level that saturated a few pixels and the concentration–gain curve was nearly flat. At low glutaraldehyde concentrations (<0.013%), the gain had to be set much higher in order to saturate a few pixels. Here, we did not observe any signal attributed to the glutaraldehyde in the pores; instead, we observed mostly background fluorescence or autofluorescence of the collagenous LC beams. At intermediate concentrations between 0.025% (×50) and 0.013% (×96), the required gain exhibited an approximately inverse linear relationship between gain and glutaraldehyde concentration. The minimum glutaraldehyde concentration that caused measurable pore fluorescence was between 0.013% and 0.016%.

Scleral Treatment With 1.25% Glutaraldehyde Treatment (Step 2). No fluorescence was observed in the pores of the LC after 5 and 15 minutes of scleral treatment with 1.25% glutaraldehyde. For these short treatment times, only background fluorescence was measured in the LC (detector gain > 900 in the periphery and center of the LC), demonstrating that

A) Overnight incubation in 0.5% glutaraldehyde
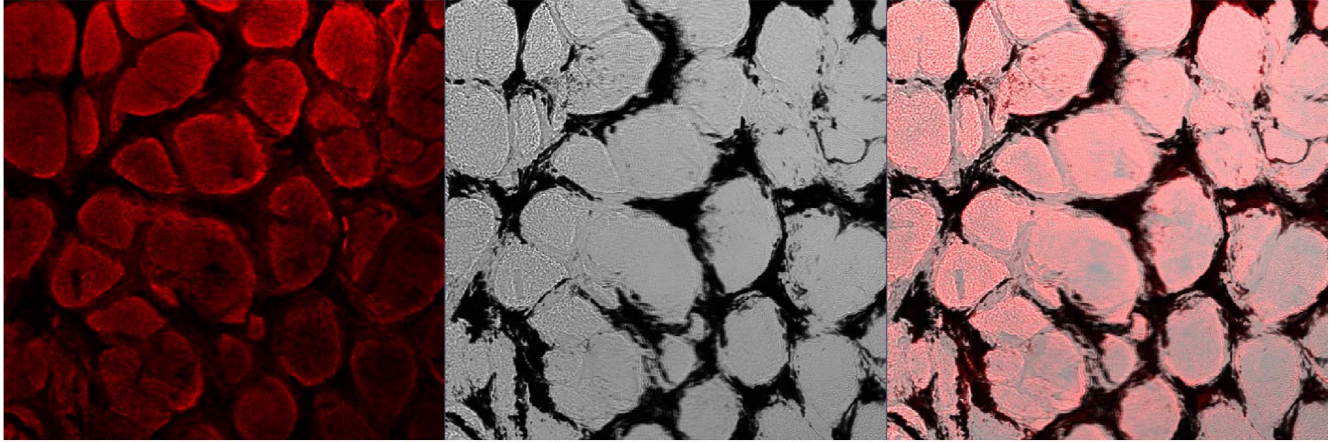
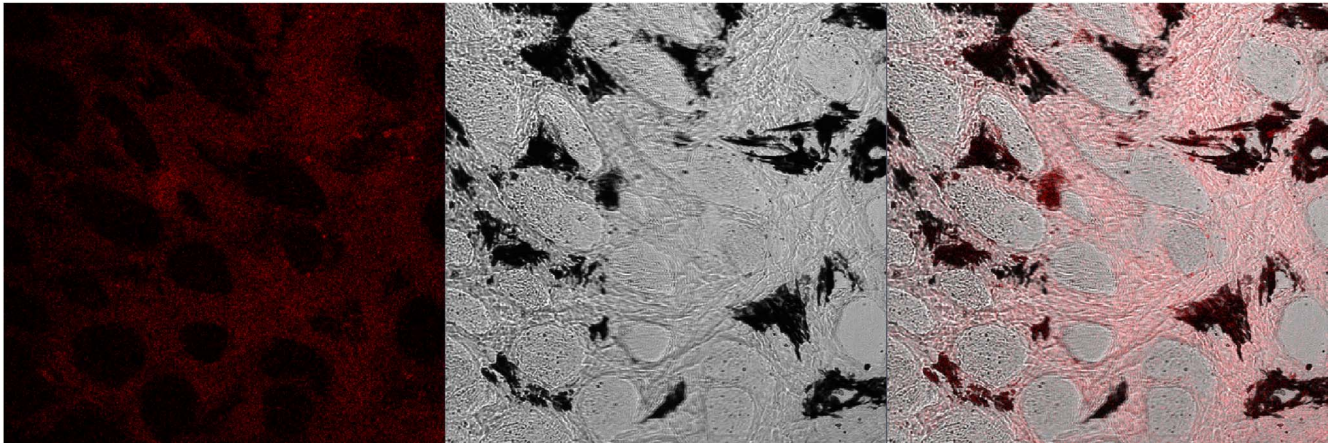## B) Overnight incubation in PBS

FIGURE 4. Confocal imaging of the LC treated with glutaraldehyde. (**A**) Specimen treated with glutaraldehyde for 14 hours. (**B**) Control specimen, incubated in PBS for 14 hours. For both, the *left column* is the fluorescence signal, the *center column* is the transmitted light image showing the beam/pore structure of the LC (*dark/light*, respectively), and the *right column* is the superimposition of the two signals. The fluorescence in glutaraldehyde-treated specimens was localized to the tissue in the pores of the LC. The gain was set to 657 in (**A**) and to 900 in (**B**). At high gains such as in (**B**), the beams of the LC autofluoresce. The *black regions* in the central images are due to pigment, commonly observed in the beams of the porcine LC.

the concentration of glutaraldehyde within the LC was uniformly lower than 0.01%. It was only after 30 minutes of scleral treatment that we detected fluorescence in the pores at the periphery of the LC, while at this same time point the central region of the LC exhibited only background levels of fluorescence. With increasing treatment time, glutaraldehyde diffused from the scleral canal to the center of the LC (Fig. 6). We determined the gain necessary to saturate a few pixels in the center and periphery of the LC and used the curve shown in Figure 5 to estimate the corresponding approximate concentration of glutaraldehyde in those regions at different time points. For treatment time shorter than 1.5 hours, the amount of autofluorescence was not different than background (gain above the threshold of 900). Autofluorescence (and hence glutaraldehyde concentration) in the periphery rose between 1.5 and 2.5 hours of treatment, while the center remained at background levels of fluorescence (gain above the threshold of 900; i.e., concentration < 0.01%) for treatment times of up to 3.5 hours. The concentration of glutaraldehyde in the periphery of the LC became greater than 0.03% after 2.5 hours. However, it was not possible to estimate the exact concentration of glutaraldehyde in the periphery of the LC

because the gain–concentration curve is nearly constant for concentrations greater than 0.03% (Fig. 5). After 6 hours of treatment, the concentration of glutaraldehyde in the center of the LC was estimated to be 0.020% (gain = 750). In these experiments, the specimens were washed in a PBS bath for 1 hour, which corresponded to the approximate time needed to perform the mechanical tests. We can safely conclude that a minimal amount of glutaraldehyde diffuses into the LC before we finish acquiring scleral and LC deformation measurements.

Quantification of Scleral Stiffening

Glutaraldehyde treatment of the peripapillary sclera caused a decrease in strain, as illustrated for one representative specimen in Figures 7A and 7B. The behavior of the porcine peripapillary sclera is nonlinear (Fig. 7C), and the relative stiffening, calculated using equation 1, was a function of the applied pressure (Fig. 7D).

On average, the glutaraldehyde-treated specimens exhibited a 44% (range, 21%–61%) reduction in first principal strain at 9 mm Hg and a 22% (range, 0%–46%) reduction in first principal strain at 38 mm Hg (Fig. 8). For all specimens, the effects of scleral stiffening on scleral deformation were larger at lower
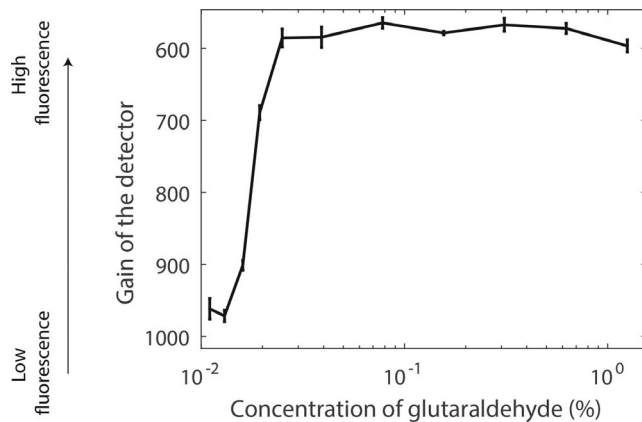
FIGURE 5. Dose–response curve for LC fluorescence after overnight incubation in solutions of glutaraldehyde of varying concentrations. The vertical axis represents the microscope gain that saturated a few pixels in the image; that is, the higher the gain, the weaker the fluorescence. At high concentration, the gain was nearly constant, corresponding to strong fluorescence from tissue in the pores, such as seen in Figure 4A. At low concentration, the gain was also uniform, but this corresponded to background fluorescence or beam autofluorescence such as seen in Figure 4B. In the transition zone, the gain linearly increased with decreasing concentration, and the fluorescence was seen in the pores.

pressures. The control specimens, left in PBS for 20 minutes, were on average between 2% (at 38 mm Hg) and 8% (at 9 mm Hg) more compliant in the second inflation test. However, the average relative stiffening was statistically not different from zero at $P > 17$ mm Hg (1-sample t-test with Bonferroni correction).

Effects of Scleral Stiffening on LC Deformation

Stiffening the peripapillary sclera resulted in a decrease in the magnitude of the three components of the principal strains in the LC, as shown in the histograms of strains (Fig. 9), the strain maps in a transverse PC μCT slice (Figs. 10C, 10D), and the average strain–pressure response over the entire LC (Fig. 10B).

At 15 mm Hg, the average relative scleral stiffening was 37% (Fig. 8, predicted from linear regression of the data shown in that figure), which corresponded to a decrease in LC deformation ranging from 26.5% to 58.1% (average = 47%, Fig. 11). The strain in the LC at 30 mm Hg was reduced between 17.8% and 53.6% (average = 39%, Fig. 11). The results were minimally affected when we used the 90th percentile LC strain instead of the average LC first principal strain to evaluate the effects of scleral stiffening on LC deformation (23.4%–

63.8% reduction at 15 mm Hg and 15.7%–61.3% reduction at 30 mm Hg).

DISCUSSION

In this study, we present experimental evidence that peripapillary scleral stiffening reduces biomechanical strain within the LC. Specifically, treating the sclera with 1.25% glutaraldehyde for 5 minutes had a direct effect on the stiffness of the sclera, causing a $43.6 \pm 13.6\%$ reduction in the maximum tensile strain in the peripapillary sclera at low pressure (9 mm Hg) and a $21.4 \pm 14.6\%$ reduction at elevated pressure (38 mm Hg). It also caused a decrease in LC deformation of $47.1 \pm 12.0\%$ at 15 mm Hg and $39.0 \pm 13.5\%$ at 30 mm Hg. We confirmed that glutaraldehyde was confined to the sclera and minimally diffused to the LC during the 5-minute treatment, and therefore the strain reduction measured in the LC following scleral stiffening was not simply due to stiffening of the LC itself.

A recent experimental study by Thornton et al.[26] evaluated the effects of glutaraldehyde treatment of the peripapillary sclera on the deformation of the ONH. In that study, the peripapillary sclera of porcine eyes was treated with a 4% glutaraldehyde solution for 30 minutes using an annular sponge, similar to our protocol. They reported an average increase in scleral stiffness of 173% at low IOP and 67% at high IOP (80 mm Hg), which is approximately three times the values measured in our experiments. Differences in treatment time and concentration most likely account for the magnitude of the effects. In the study by Thornton et al.,[26] the stiffness of the LC was not altered by the treatment, confirming that glutaraldehyde did not diffuse into the LC within 30 minutes. They used a low-resolution optical method to measure strains in the LC and reported a large decrease in tensile strain in the LC from 10.2% to 0%, although the authors stated a lack of confidence in the sensitivity of their method to measure small deformations. This study extends the previous work of Thornton et al.,[26] by direct, relatively high-accuracy experimental measurement of strains in the LC after scleral stiffening.

Previous finite element (FE) modeling studies also predicted that a larger scleral stiffness would cause a decrease in LC tensile strain when all the other parameters were held constant (e.g., eye geometry, material properties of all other tissues).[15] For instance, using the applet (http://www. ocularbiomechanics.com/Software.html) created by Sigal,[15] we can predict that a 40% increase in scleral modulus (from 3 to 4.2 MPa) would cause the median first principal strain in the LC to decrease from 1.10% to 0.90% at 15 mm Hg (all other parameters held at their default values), which corresponds to a relative LC strain reduction of 18%. The median relative scleral stiffening measured in our experiments at 15 mm Hg
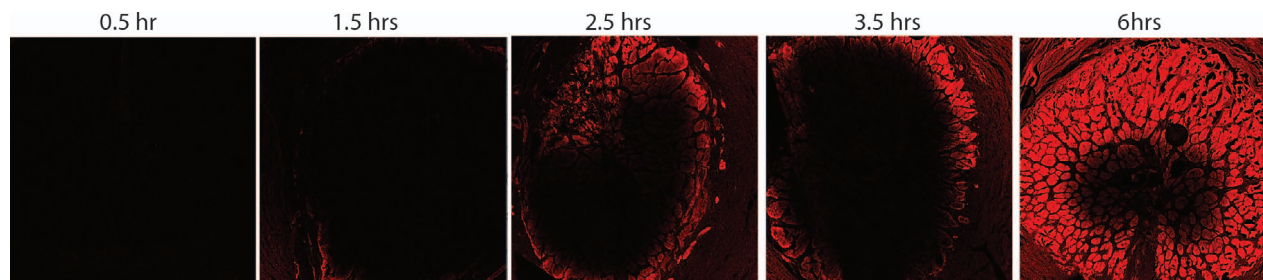

FIGURE 6. LC fluorescence due to peripapillary scleral treatment with 1.25% glutaraldehyde. Fluorescence microscopy image of the central slice of the LC for different durations of scleral treatment (indicated on *top* of each image). The parameters of the microscope were identical for all images (tile scan 6 × 6 images, detector gain = 700, pixel averaging = 4). Because the same gain was used to generate the five images, the regions with concentrations of glutaraldehyde larger than 0.03% are saturated. However, these images illustrate the time-dependent diffusion of glutaraldehyde from the periphery to the center of the LC.
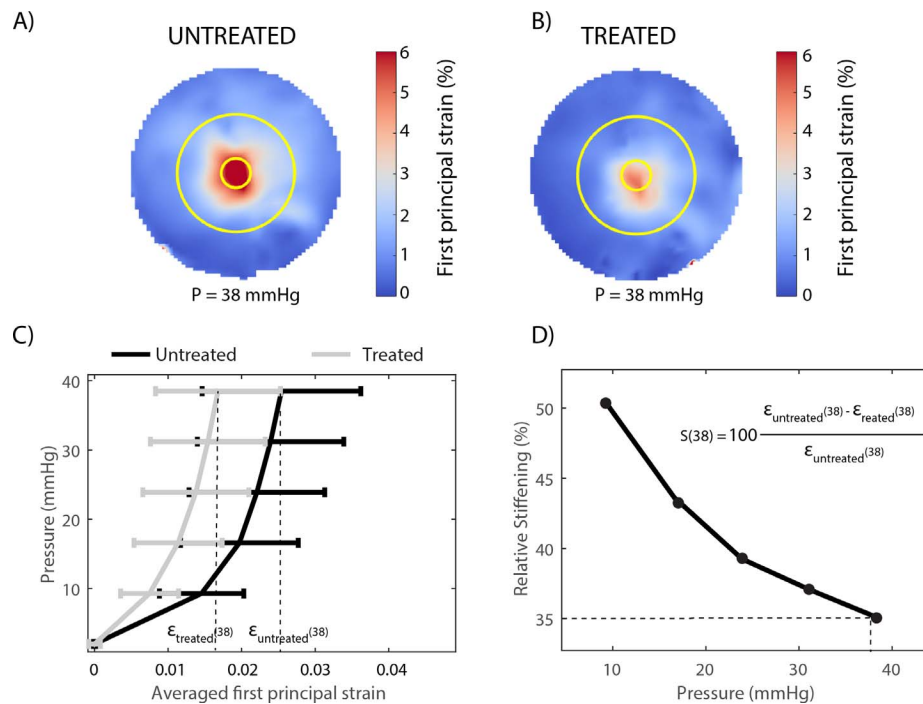
Investigative Ophthalmology & Visual Science

FIGURE 7. Experiment A: Glutaraldehyde treatment of the sclera caused a pressure-dependent decrease in the magnitude of the peripapillary scleral deformation, illustrated here for one specimen. (**A**) Map of the first principal strain (maximum tensile deformation) determined at 38 mm Hg before treatment. (**B**) Map of the first principal strain determined at the same pressure after treatment. In (**A**) and (**B**), the two *circles* ($r = 1.5$ mm and $r = 6$ mm) delineate the inner and outer contours of the peripapillary scleral region where strains were averaged to estimate the relative scleral stiffening. (**C**) Pressure versus averaged first principal strain before treatment (*gray*) and after treatment (*black*), quantifying the reduction in first principal strain caused by glutaraldehyde treatment at each pressure step. The *error bars* represent the standard deviation of the first principal strain over the entire peripapillary sclera region. (**D**) The relative scleral stiffening for this specimen was calculated using equation 1 and is plotted as a function of the applied pressure. The calculation of the relative stiffening is illustrated at 38 mm Hg (*dashed lines*).
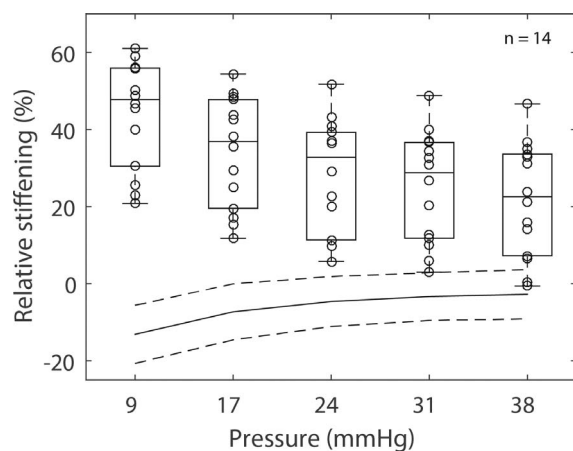

FIGURE 8. Experiment A: box plot of the relative scleral stiffening caused by a 5-minute treatment of the peripapillary sclera with a 1.25% glutaraldehyde solution. Scleral stiffening was calculated at five levels of IOPs between 9 and 38 mm Hg using equation 1. The scatter plot superimposed on each box plot represents individual specimens ($n = 14$). The *solid line* and the *dashed lines* represent the average and average ± standard deviation of the relative stiffening calculated for six specimens left in PBS (i.e., not subjected to glutaraldehyde treatment of the peripapillary sclera). For those specimens, the average relative stiffening was not different from zero at $P > 17$ mm Hg (adjusted P value > 0.01). The average stiffening was always significantly different from zero for the treated specimens (adjusted P value < 0.001).

($\sim$40%) was associated with a LC strain reduction of 26.5% to 58.1%, which is slightly larger than what was predicted by the FE models. Differences in geometry (porcine eye versus human), material behavior (nonlinear for the porcine eye versus linear for the human eye), or eye stiffness (LC strains in the order of 3% to 5% for the porcine eye and 1% for the human eye at 15 mm Hg) may account for the observed differences.

Although our findings demonstrate that stiffening the peripapillary sclera reduces the IOP-induced mechanical strains in the LC, it remains to be shown that scleral stiffening is neuroprotective in glaucoma. Glaucoma is a multifactorial disease, in which a combination of mechanical, vascular, and biochemical events occur simultaneously. We postulate that shielding the LC from excessive deformation will decrease the magnitude of mechanical events such as the direct mechanical insults to the axons or the mechanosensitive activation of astrocytes. However, it may also have detrimental effects on blood flow or phenotypic expression of other cell types. In fact, a recent study by Kimball et al.[22] reported increased axonal loss in mice with induced ocular hypertension whose sclera had been stiffened with glyceraldehyde. In that study, the entire globe was exposed to three injections of glyceraldehyde, which caused an average relative scleral stiffening of 50% at 15 mm Hg and 55% at 30 mm Hg. We suggest that constraining the treatment zone to the peripapillary sclera and using a relatively low concentration of the stiffening solution may decrease the magnitude of the mechanical events without altering the vascular or biochemical response of the ONH. Further computational modeling and animal studies controlling the extent of the treatment zone and the magnitude of the stiffening will be important to elucidate the neuroprotective role of increased scleral stiffness in glaucoma.
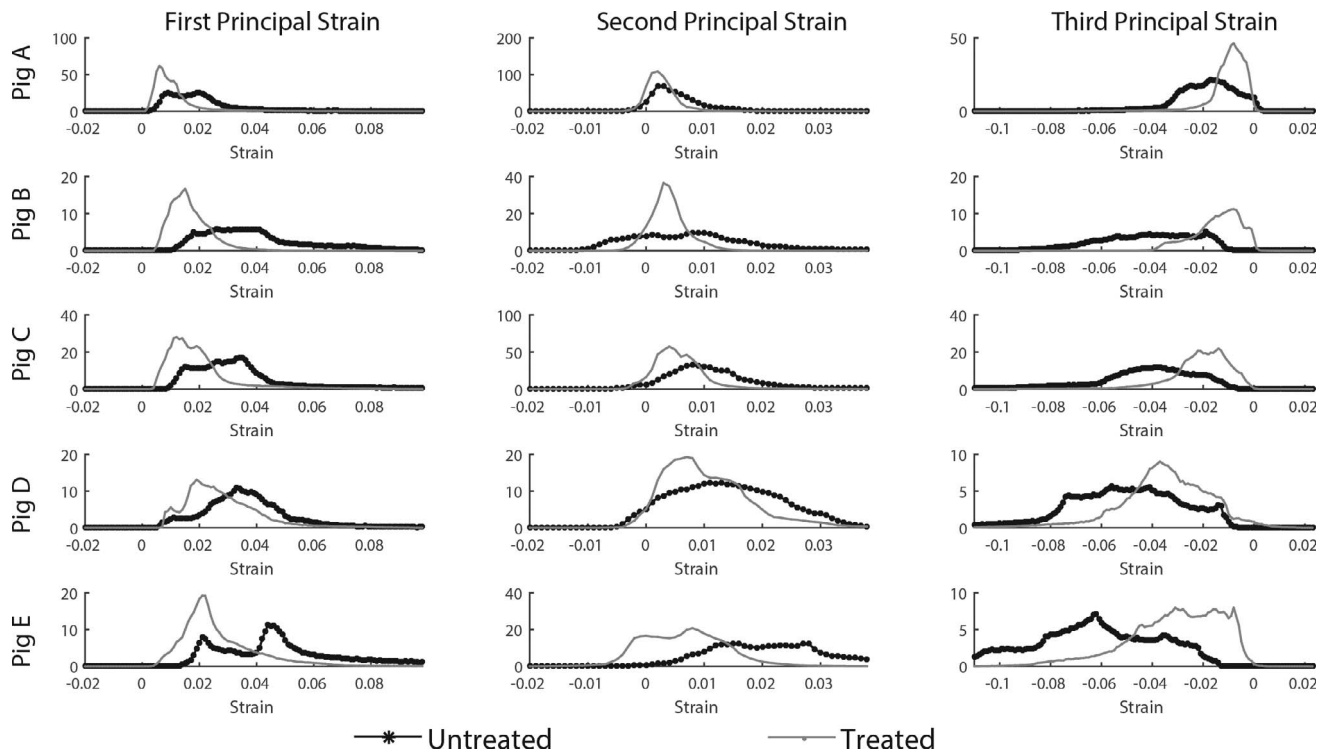
FIGURE 9. Experiment B: LC principal strain histograms at 15 mm Hg before and after scleral stiffening for the five specimens of this study. Strains were computed with digital volume correlation (with respect to the reference configuration at 4 mm Hg). The vertical axis of each histogram is the total volume of LC tissue subjected to a given strain level. Note that the *y*-axis scale is different between specimens, due to subject-to-subject variations in LC size. All principal strain histograms were shifted toward zero after scleral treatment with glutaraldehyde, indicating a reduction in deformation of the tissue of the LC after scleral stiffening.

Several limitations should be considered when interpreting the results of this study. The results of experiments A and B are not directly comparable. We did not use the same eyes to measure the effects of glutaraldehyde treatment on scleral stiffness (experiment A) and on LC deformation (experiment B) because the two experiments were not performed in the same location. The age of the animals differed between the two experiments (24 vs. 5 months old), which may have affected the magnitude of the strains measured. Experimental studies have shown that the sclera becomes stiffer with age.[38,39] The eyes of the young animals used for measuring LC deformation were smaller, and it is possible that a larger proportion of the sclera was stiffened in this experiment. This may explain why we observed a larger strain reduction in the LC than in the sclera. The diffusion experiments were performed using eyes of older animals. Younger animals were smaller and probably had a thinner sclera. Assuming that the concentration of glutaraldehyde follows the classical unsteady diffusion equation, the concentration of delivered glutaraldehyde would be larger in the sclera of younger eyes with thinner scleras. For example, the same concentration would be observed in an eye of scleral thickness T at time t as in an eye of thickness $\frac{1}{2} T$ at time $\frac{1}{4} t$. Since we did not observe fluorescence at 20 minutes in the older eye, we conclude that the concentration of glutaraldehyde in the young sclera was also low at 5 minutes. Further, the pressure loading regimens were different between experiments A and B. In experiment A, we measured the instantaneous response of the sclera (quasi-continuous pressure increase). In experiment B, we measured the equilibrium response of the LC as the pressure was maintained for 15 minutes before deformation measurements to prevent motion artifacts in the scans.

Second, glutaraldehyde is cytotoxic. Other biocompatible agents should be tested for their efficiency to cross-link scleral collagen. We chose glutaraldehyde because it was shown to be the most efficient and fastest chemical to stiffen the porcine and human sclera.[25] Our PC μCT method relies on access to a synchrotron light source, which is necessarily limited by high facility cost and demand. Fast stiffening of the sclera allowed us to increase the number of experiments we could perform during our time-limited visit to the Diamond Light Source. In collagen-rich tissues such as the sclera, the mechanical response at low pressure is dominated by the response of the proteoglycan-rich matrix, while the crimped (wavy) collagen fibers have a lesser contribution to the tissue stress response. As pressure increases, collagen fibers uncrimp and progressively carry more load, which causes the sclera to exhibit a typical stiffening response as shown in Figure 7C. Our findings showed that the relative stiffening was larger at low pressures (Fig. 8), suggesting that glutaraldehyde treatment has a greater effect on the material properties of the matrix than on the material properties of the collagen fibers. We note that the aqueous glutaraldehyde at room temperature could have vaporized and cross-linked regions of the sclera or the ON that we did not intend to cross-link.[40] However, the effects would be minimal in the LC, which is not exposed to air. We also expect vapor fixation to have had a negligible effect on the overall stiffness of the posterior sclera due to the short treatment time of 5 minutes.

Digital image correlation and DVC are subject to similar limitations in their ability to resolve small deformation, as discussed in Coudrillier et al.[28,32] The deformation in the treated porcine peripapillary sclera varied between 1% and 3%, and the deformation in the treated LC varied between 2% and 5%, which is at least two orders of magnitude larger than the
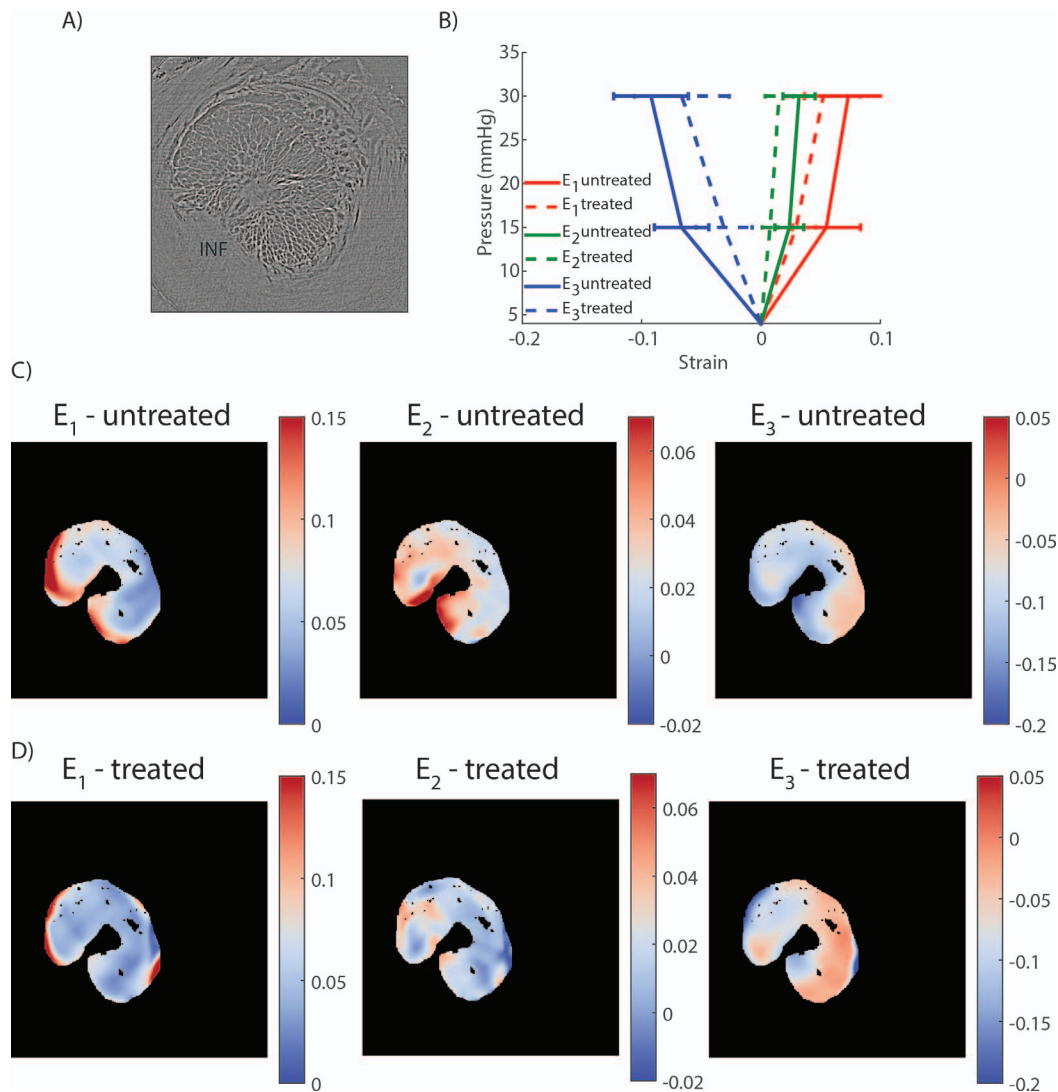
FIGURE 10. Experiment B: digital volume correlation for strain calculation. (**A**) Transverse slice (i.e., perpendicular to the optic nerve axis) through the PC µCT scan volume acquired at 4 mm Hg. (**B**) Average and standard deviation of the first, second, and third principal strains (E_1, E_2, and E_3, respectively) over the slice shown in (**A**) computed with DVC and plotted versus the applied pressure. All three principal strains were lower in the treated specimen at both pressures. (**C**) Maps of the first, second, and third principal strain at 30 mm Hg in the untreated specimens. (**D**) Maps of the first, second, and third principal strain at 30 mm Hg in the treated specimens. In (**C**) and (**D**), the regions outside the LC (sclera, ventral groove, pial septa) and within the LC with a correlation value lower than 0.70 were masked and appear in *black*. The inferior (INF) pole is indicated in [**A**]. Similar results were obtained in other transverse slices.

minimal strains DIC and DVC can resolve. Therefore, we are confident that our strain measurements were not limited by the resolution of DIC or DVC.

Lastly, we presented average strains over the entire LC volume. How the regional deformation profiles were affected by glutaraldehyde treatment was not evaluated in this study but may be of importance. For instance, we could imagine a scenario in which the average LC deformation was reduced by treatment while at the same time small LC regions experienced more deformation than the maximum deformation seen in the untreated LC. If elevated peak strains in LC tissue drove axonal degeneration in glaucoma, this scenario would have a detrimental effect on vision. However, the histograms of strains presented in Figure 9 seem to indicate that this scenario is also unlikely. Specifically, although the shape of the histogram was not entirely identical in the treated and untreated specimens, the maximum first and second principal strains over the entire LC, which are measures of the local in-

plane tensile deformation of the LC, were always lower in the treated specimens, indicating that no region of the LC was subjected to more stretch after treatment than the most stretched region of the untreated LC. Similarly, the third principal strain, a measure of the compression of the tissue, always had lower magnitude in the treated specimens, indicating that treatment reduced the peak compressive insult to the LC axons and cells. This finding suggests that peripapillary scleral stiffening decreases LC peak strains, and therefore may be beneficial in glaucoma. It should also be noted that we did not analyze the directions of principal strains. We have shown in a previous paper[28] that first and second principal strain directions were largely aligned with the in-plane direction of the posteriorly bowed LC, while the third principal strain direction was largely parallel to the thickness direction. How strain directions were affected by treatment was not within the scope of this work and will be analyzed in future studies.
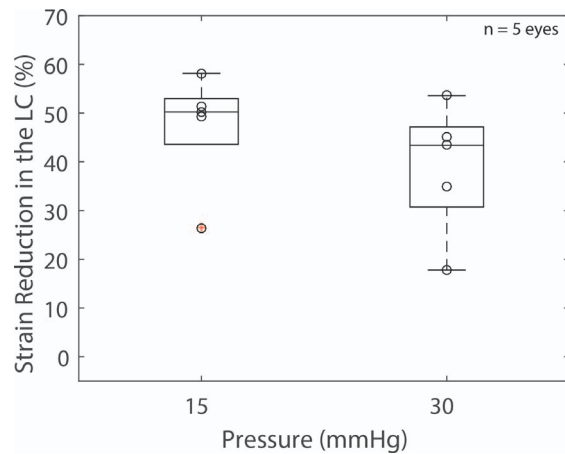
Figure 11. Experiment B: box plot of the reduction in strain in the LC caused by a 5-minute treatment of the peripapillary sclera with a 1.25% glutaraldehyde solution at two levels of imposed pressures. Peripapillary scleral stiffening caused a decrease in LC deformation. The scatter plot superimposed on each box plot represents individual specimens ($n = 5$).

In conclusion, we demonstrated that a moderate increase in scleral stiffness (~10%–60%) was associated with a 25% to 76% decrease in LC strains. Further studies should be conducted to elucidate the neuroprotective role of scleral stiffening in glaucoma.

References

1. Quigley HA, Broman AT. The number of people with glaucoma worldwide in 2010 and 2020. *Br J Ophthalmol*. 2006;90:262–267.

2. Heijl A, Leske MC, Bengtsson B, et al. Reduction of intraocular pressure and glaucoma progression: results from the Early Manifest Glaucoma Trial. *Arch Ophthalmol*. 2002;120:1268–1279.

3. Leske MC, Heijl A, Hussein M, et al. Factors for glaucoma progression and the effect of treatment: the early manifest glaucoma trial. *Arch Ophthalmol*. 2003;121:48–56.

4. Noecker RJ. The management of glaucoma and intraocular hypertension: current approaches and recent advances. *Ther Clin Risk Manag*. 2006;2:193–206.

5. Burgoyne CF, Downs JC, Bellezza AJ, Suh JK, Hart RT. The optic nerve head as a biomechanical structure: a new paradigm for understanding the role of IOP-related stress and strain in the pathophysiology of glaucomatous optic nerve head damage. *Prog Retin Eye Res*. 2005;24:39–73.

6. Campbell IC, Coudrillier B, Ross Ethier C. Biomechanics of the posterior eye: a critical role in health and disease. *J Biomech Eng*. 2014;136:021005.

7. Anderson DR, Hendrickson A. Effect of intraocular pressure on rapid axoplasmic transport in monkey optic nerve. *Invest Ophthalmol Vis Sci*. 1974;13:771–783.

8. Sigal IA, Grimm JL, Jan NJ, Reid K, Minckler DS, Brown DJ. Eye-specific IOP-induced displacements and deformations of human lamina cribrosa. *Invest Ophthalmol Vis Sci*. 2014;55:1–15.

9. Beckel JM, Argall AJ, Lim JC, et al. Mechanosensitive release of adenosine 5′-triphosphate through pannexin channels and mechanosensitive upregulation of pannexin channels in optic nerve head astrocytes: a mechanism for purinergic involvement in chronic strain. *Glia*. 2014;62:1486–1501.

10. Rogers RS, Dharsee M, Ackloo S, Sivak JM, Flanagan JG. Proteomics analyses of human optic nerve head astrocytes following biomechanical strain. *Mol Cell Proteomics*. 2012;11:M111.012302.

11. Girard MJ, Dupps WJ, Baskaran M, et al. Translating ocular biomechanics into clinical practice: current state and future prospects. *Curr Eye Res*. 2015;40:1–18.

12. Strouthidis NG, Girard MJ. Altering the way the optic nerve head responds to intraocular pressure-a potential approach to glaucoma therapy. *Curr Opin Pharmacol*. 2013;13:83–89.

13. Quigley HA, Cone FE. Development of diagnostic and treatment strategies for glaucoma through understanding and modification of scleral and lamina cribrosa connective tissue. *Cell Tissue Res*. 2013;353:231–244.

14. Sigal IA, Flanagan JG, Ethier CR. Factors influencing optic nerve head biomechanics. *Invest Ophthalmol Vis Sci*. 2005;46:4189–4199.

15. Sigal IA. An applet to estimate the IOP-induced stress and strain within the optic nerve head. *Invest Ophthalmol Vis Sci*. 2011;52:5497–5506.

16. Coudrillier B, Boote C, Quigley HA, Nguyen TD. Scleral anisotropy and its effects on the mechanical response of the optic nerve head. *Biomech Model Mechanobiol*. 2013;12:941–963.

17. Nguyen C, Cone FE, Nguyen TD, et al. Studies of scleral biomechanical behavior related to susceptibility for retinal ganglion cell loss in experimental mouse glaucoma. *Invest Ophthalmol Vis Sci*. 2013;54:1767–1780.

18. Downs JC, Suh JK, Thomas KA, Bellezza AJ, Hart RT, Burgoyne CF. Viscoelastic material properties of the peripapillary sclera in normal and early-glaucoma monkey eyes. *Invest Ophthalmol Vis Sci*. 2005;46:540–546.

19. Girard MJ, Suh JK, Bottlang M, Burgoyne CF, Downs JC. Biomechanical changes in the sclera of monkey eyes exposed to chronic IOP elevations. *Invest Ophthalmol Vis Sci*. 2011;52:5656–5669.

20. Coudrillier B, Pijanka JK, Jefferys JL, et al. Glaucoma-related changes in the mechanical properties and collagen microarchitecture of the human sclera. *PLoS One*. 2015;10:e0131396.

21. Hommer A, Fuchsjager-Mayrl G, Resch H, Vass C, Garhofer G, Schmetterer L. Estimation of ocular rigidity based on measurement of pulse amplitude using pneumotonometry and fundus pulse using laser interferometry in glaucoma. *Invest Ophthalmol Vis Sci*. 2008;49:4046–4050.

22. Kimball EC, Nguyen C, Steinhart MR, et al. Experimental scleral cross-linking increases glaucoma damage in a mouse model. *Exp Eye Res*. 2014;128:129–140.

23. Wollensak G, Spoerl E, Seiler T. Riboflavin/ultraviolet-a-induced collagen crosslinking for the treatment of keratoconus. *Am J Ophthalmol*. 2003;135:620–627.

24. Dotan A, Kremer I, Livnat T, Zigler A, Weinberger D, Bourla D. Scleral cross-linking using riboflavin and ultraviolet-a radiation for prevention of progressive myopia in a rabbit model. *Exp Eye Res*. 2014;127:190–195.

25. Wollensak G, Spoerl E. Collagen crosslinking of human and porcine sclera. *J Cataract Refract Surg*. 2004;30:689–695.

26. Thornton IL, Dupps WJ, Roy AS, Krueger RR. Biomechanical effects of intraocular pressure elevation on optic nerve/lamina cribrosa before and after peripapillary scleral collagen crosslinking. *Invest Ophthalmol Vis Sci*. 2009;50:1227–1233.

27. Girard M, Suh JK, Hart RT, Burgoyne CF, Downs JC. Effects of storage time on the mechanical properties of rabbit peripapillary sclera after enucleation. *Curr Eye Res*. 2007;32:465–470.

28. Coudrillier B, Geraldes D, Vo N, et al. Phase-contrast microcomputed tomography measurements of the intraocular pressure-induced deformation of the porcine lamina cribrosa. *IEEE Trans Med Imaging*. 2015;35:988–999.

29. Tonge TK, Murienne BJ, Coudrillier B, Alexander S, Rothkopf W, Nguyen TD. Minimal preconditioning effects observed for inflation tests of planar tissues. *J Biomech Eng*. 2013;135: 114502.

30. Collins JS, Goldsmith TH. Spectral properties of fluorescence induced by glutaraldehyde fixation. *J Histochem Cytochem*. 1981;29:411–414.

31. Myers KM, Coudrillier B, Boyce BL, Nguyen TD. The inflation response of the posterior bovine sclera. *Acta Biomater*. 2010; 6:4327–4335.

32. Coudrillier B, Tian J, Alexander S, Myers KM, Quigley HA, Nguyen TD. Biomechanics of the human posterior sclera: age- and glaucoma-related changes measured using inflation testing. *Invest Ophthalmol Vis Sci*. 2012;53:1714–1728.

33. Pyne JD, Genovese K, Casaletto L, Vande Geest JP. Sequential-digital image correlation for mapping human posterior sclera and optic nerve head deformation. *J Biomech Eng*. 2014;136: 021002.

34. Atwood RC, Bodey AJ, Price SW, Basham M, Drakopoulos M. A high-throughput system for high-quality tomographic reconstruction of large datasets at Diamond Light Source. *Philos Trans A Math Phys Eng Sci*. 2015;373:20140398.

35. Vo NT, Drakopoulos M, Atwood RC, Reinhard C. Reliable method for calculating the center of rotation in parallel-beam tomography. *Opt Express*. 2014;22:19078–19086.

36. Sukjamsri C, Geraldes DM, Gregory T, et al. Digital volume correlation and micro-CT: an in-vitro technique for measuring full-field interface micromotion around polyethylene implants. *J Biomech*. 2015;48:3447–3454.

37. Diez-Fraile A, Van Hecke N, Guérin CJ, D'Herde K. Optimizing multiple immunostaining of neural tissue. In: Dehghani H, ed. *Applications of Immunocytochemistry*. InTech; 2012:345–442.

38. Coudrillier B, Pijanka J, Jefferys J, et al. Collagen structure and mechanical properties of the human sclera: analysis for the effects of age. *J Biomech Eng*. 2015;137:041006.

39. Girard MJ, Suh JK, Bottlang M, Burgoyne CF, Downs JC. Scleral biomechanics in the aging monkey eye. *Invest Ophthalmol Vis Sci*. 2009;50:5226–5237.

40. Zhang Y, Venugopal J, Huang Z-M, Lim C, Ramakrishna S. Crosslinking of the electrospun gelatin nanofibers. *Polymer*. 2006;47:2911–2917.

Investigative Ophthalmology & Visual Science